[CANCER RESEARCH 63, 9042–9047, December 15, 2003]

Identification of Prognostic Markers in Bone Sarcomas Using Proton-Decoupled Phosphorus Magnetic Resonance Spectroscopy

Kristen L. Zakian,[1,3] Amita Shukla-Dave,[1,3] Paul Meyers,[2] Richard Gorlick,[2] John Healey,[4] Howard T. Thaler,[5] Andrew G. Huvos,[7] David M. Panicek,[3] and Jason A. Koutcher[1,3,6]

Department of [1]Medical Physics, [2]Pediatrics, [3]Radiology, [4]Orthopedic Surgery, [5]Biostatistics, [6]Medicine, and [7]Pathology, Memorial Sloan-Kettering Cancer Center, New York, New York

ABSTRACT

It has been hypothesized that the ^{31}Phosphorus (^{31}P) nuclear magnetic resonance spectrum from certain tumors may provide prognostic information. The goal of the present study was to identify prognostic metabolic markers by using proton-decoupled phosphorus magnetic resonance spectroscopic imaging (^{31}P MRSI). Twenty patients with bone [osteogenic (OS) and Ewing's (ES) and/or primitive neuroectodermal tumor (PNET)] sarcoma, treated with chemotherapy and surgery or with chemotherapy alone, underwent ^{31}P MRSI studies pre- and post-therapy. The studies were performed on a 1.5 Tesla General Electric (GE) clinical scanner equipped with a stand-alone proton decoupler and a dual ^{1}H/^{31}P surface coil pair. The limited sensitivity of the ^{31}P nucleus required that a large soft tissue component of the disease be located within 10 cm (maximum distance) of the body surface and the use of a highly sensitive coil placed near the skin surface. Proton decoupling and nuclear Overhauser enhancement were used to improve the spectral resolution and signal:noise ratio. Baseline ^{31}P spectral features and metabolic changes with treatment were compared with treatment outcome. The patients were categorized depending on survival as event-free survivors or those who died. The pretreatment nucleoside triphosphate:inorganic phosphate (NTP:P_i) ratio, an index of tumor bioenergetic status, was significant ($P = 0.003$) in differentiating event-free survivors *versus* those who died. The pretreatment NTP:P_i was higher in patients who were destined to undergo a durable event-free survival compared with those who died. The results are promising, although a prospective study is necessary for confirmation. ^{31}P MRSI appears to be a useful tool for the prediction of survival before therapy in bone sarcomas.

INTRODUCTION

Primary bone tumors are the third most common tumors in adolescents and young adults (1–3). Of these, osteosarcoma (OS) occurs most frequently, accounting for 35% of all primary sarcomas of bone and 56% of the malignant bone tumors in the first two decades of life (1, 2). Ewing's sarcoma (ES), the second most common primary bone cancer, accounts for ~30% of all primary bone tumors. Before the development of adjuvant/neoadjuvant chemotherapy, even localized potentially curable bone tumors had a greater than 80% mortality rate. Multi-agent chemotherapy has resulted in cures for a significant percentage of patients but there are still failures (~30–50%; Refs. 4, 5). In addition, chemotherapy is associated both with the development of drug-resistant clones and with toxicity. An early predictor of response to chemotherapy would be extremely valuable, allowing the oncologist to intervene with alternative therapies.

In OS, the absence of metastases at initial staging is the most important prognostic indicator at present. In patients with localized ES or OS who undergo neo-adjuvant chemotherapy, the most reliable prognostic factor is response to treatment (percentage necrosis) as assessed by a pathologist at the time of surgery (5, 6). However, histological response, by current definition, cannot be known before or during neo-adjuvant treatment. In addition, adjuvant chemotherapy given to patients with a poor histological response measured after surgery did not improve outcome, emphasizing the need for an *a priori* response predictor. Other prognostic factors are tumor size and site of tumor (related to resectability) in OS and to a lesser extent in ES, but these factors are not strong enough to allow stratification or individualization of treatment (7, 8). Patient age, tumor proliferation rate, and the presence of p53 may also affect outcome (7, 8). The p53 pathway inactivation is a strong prognostic factor in ES but is only present in 30% of patients, limiting its utility (7, 8). Thus, in bone sarcomas, a clear need exists to identify a prognostic indicator that would help in selecting poor-risk patients before exposure to ineffective chemotherapy for consideration of novel treatment paradigms. Alternatives to standard chemotherapy regimens, such as ifosfamide and etoposide for OS, or high-dose ifosfamide (wherein there are data to suggest a dose-response relationship), could be considered.

There is evidence that tumor metabolic parameters may provide prognostic information. Recent studies have suggested that measurements of tumor hypoxia by oxygen electrodes may predict patient outcome and the likelihood of metastatic disease in certain tumors (9, 10). It has also been shown that the measurement of tumor lactate can provide prognostic information before treatment (11). Thus, noninvasive measures of tumor metabolism may potentially be useful for predicting prognosis. Phosphorus magnetic resonance spectroscopic imaging (^{31}P MRSI) is a noninvasive technique that can provide information on tumor energy status, membrane metabolism, and pH. In studies of non-Hodgkin's lymphomas (12), head and neck cancers (13), and soft tissue sarcomas (14–18), there is evidence that the ^{31}P nuclear magnetic resonance (NMR) spectrum may provide prognostic information. The present study characterizes the ^{31}P NMR spectrum in untreated bone sarcomas and attempts to assess its prognostic value.

MATERIALS AND METHODS

Patients included in the study had a biopsy-proven diagnosis of bone sarcoma, either OS or ES/primitive neuroectodermal tumor, before study. The limited sensitivity of the ^{31}P nucleus requires the use of a highly sensitive resonator placed on the surface of the patient near the tumor; therefore, in general, a mass of $3 \times 3 \times 3$ cm or larger, located within 10 cm (maximum distance) of the body surface, was necessary for patient inclusion in the study. Additionally, prior imaging studies were reviewed to determine whether the lesion had an associated extraosseous soft tissue component that was deemed necessary for generating an adequate NMR signal. All of the patients had the baseline ^{31}P MRSI performed between day 0 to day 10 (average, 4 ± 1 day) before the start of chemotherapy. All of the subjects or their legal guardians signed informed consent as approved by the Institutional Review Board.

MR Spectroscopy. All of the data were obtained on a 1.5 Tesla General Electric [(GE) Milwaukee, WI] Signa Horizon scanner equipped with a stand-alone proton decoupler. The patient examination consisted of proton imaging followed by proton-decoupled ^{31}P MRSI. Pre-spectroscopic imaging consisted of spin-spin relaxation (T_2)-weighted, fat-suppressed scout imaging in the axial plane using the whole-body coil. A radiologist identified the most viable-

Received 6/6/03; revised 10/10/03; accepted 10/14/03.

Grant support: National Cancer Institute Grant R01CA65959 and Grant CA05826.

The costs of publication of this article were defrayed in part by the payment of page charges. This article must therefore be hereby marked *advertisement* in accordance with 18 U.S.C. Section 1734 solely to indicate this fact.

Note: K. L. Zakian and A. Shukla-Dave contributed equally to this work.

Requests for reprints: Kristen L. Zakian, Department of Medical Physics, Memorial Sloan-Kettering Cancer Center, 1275 York Avenue, New York, NY 10021. E-mail: zakiank@mskcc.org.

appearing region within the soft tissue component of the tumor. The criteria used were: (*a*) avoidance of necrotic areas; and (*b*) selection of a voxel as close to the coil as possible but excluding normal tissue. A dual ^{1}H-^{31}P coil pair (Intermagnetics General Corporation; Medical Advances, Milwaukee, WI) was then placed adjacent to this optimal tumor site. This resonator pair consisted of a 12-cm square ^{31}P resonator comounted with a flexible two-loop proton coil. With this coil pair in place, T_2-weighted, fat-suppressed, fast-spin echo imaging of the tumor was performed in two orthogonal planes (repetition time = 4000 ms; echo time = 102 ms; echo-train length = 12; averages = 2). ^{31}P MRSI consisted of three-dimensional chemical shift imaging (19) using hard radiofrequency pulses with the following parameters: phase-encode matrix = 8 × 8 × 8; field of view = 24, 28, or 32 cm; repetition time = 1 s; signal averages = 4; sampled points = 1024; spectral width = 8000 Hz; flip angle = ~45°; scan time = 34 min. The flip angle was calibrated using a triphenylphosphite standard mounted on the center of the ^{31}P coil. Waltz 4 proton decoupling was applied during data acquisition and low-level continuous wave power was applied in the remainder of the TR interval to maintain the nuclear Overhauser enhancement. Fiducial markers on the coil permitted retrospective assessment of the coil position in space for field mapping.

Spectroscopic Data Processing. *In vivo* NMR data were processed using SAGE/IDL (General Electric, Milwaukee, WI; Research Systems Incorporated, Boulder, CO) for voxel shifting, spatial Fourier transform, and single-voxel free induction decay extraction. The single-voxel location was chosen retrospectively to include as much viable (non-necrotic) soft tissue component as possible. However, some malignant bone component was included in the majority of studies. The percentage of the voxel composed of soft tissue was estimated by assessing the voxel in three consecutive axial images. Once the tumor free induction decay was extracted from the three-dimensional data set, Lorentzian peak areas were fit in the time domain using MRUI-AMARES software (20) and/or jMRUI (21). From the raw peak areas, the following ratios were tabulated: PE:NTP, PE:PC, PME:NTP, PDE:NTP, PDE:PME, and NTP:P_i, where PE = phosphoethanolamine, PC = phosphocholine, PME = phosphomonoester, PDE = phosphodiester, P_i = inorganic phosphate, and NTP = nucleoside triphosphate. These ratios were selected based on data in the literature that suggested they may have some prognostic value (14–18). In addition to raw peak area ratios, normalized individual metabolite quantities relative to the triphenylphosphite standard were also calculated from the metabolite peak areas in each spectrum. For these calculations, software was written in IDL for performing Biot-Savart B_1 calculations and overlaying the three-dimensional B_1 field map on the images for calculation of the distribution of B_1 intensity and flip angle. Peak areas were corrected for: (*a*) saturation using the calculated three-dimensional flip angle map and published spin-lattice relaxation (T_1) values for normal muscle (22); and (*b*) receive sensitivity over the voxel relative to the standard (23). Metabolite levels relative to the standard are reported as normalized units (n.u.). No corrections were made for nuclear Overhauser enhancement or point spread function. Intracellular pH was calculated from the P_i:α-NTP chemical shift in the spectrum using a calibration curve generated in this laboratory.

Patient Selection. ^{31}P MRSI studies were carried out before the onset of treatment in 36 bone sarcoma patients after the methodology was fully standardized. Five patients were unable to complete the exam because of discomfort or claustrophobia. Data from 10 patients were discarded because of inadequate signal:noise ratio in 5 cases and technical failure in 5 cases. One patient had treatment-related mortality and was, therefore, inevaluable for response. The remaining 20 patients included 11 ES/primitive neuroectodermal tumor and 9 OS. The clinical characteristics of these patients are included in Table 1. None of these patients had received any prior treatment for their disease.

Sixteen patients were treated with chemotherapy followed by surgery, whereas 4 patients had chemotherapy only and did not undergo surgery because of progressive disease and distant metastases. Patients were followed for a range of 8 to 69 months (average follow-up, 38 ± 5 months). Clinical follow-up to detect metastatic disease or local failure included physical examination, computed tomography, bone scan, and magnetic resonance imaging. Patients were grouped according to survival as either event-free survivors (EFSs) or those who died. EFSs were patients who obtained a complete remission and remained in that state at the time the data were analyzed. Patients who did not respond or progressed on chemotherapy, or relapsed within 6 months after surgery, or had distant metastatic disease after chemotherapy and did not undergo surgery, all died shortly thereafter. In the category of EFSs, two ES/primitive neuroectodermal tumor patients had radiation therapy for close margins after chemotherapy and surgery and one OS patient had radiation therapy (to the lungs) after chemotherapy and surgery for possible lung metastasis. In the group of those who died, three ES patients received palliative radiation therapy after failure.

Table 1 *Clinical characteristics of 20 bone sarcoma patients*

Patient no.	Age (yr)	Sex	Diagnosis (surgical/ pathological)	Pathological response grade no.[a]	Outcome
1	18	F	Ewing/PNET[b]	III	Dead[c]
2	12	M	Ewing/PNET	IV	Event-free survivor[d]
3	6	M	Ewing/PNET	I	Event-free survivor
4	15	M	Ewing/PNET	IV	Dead
5	13	F	Ewing/PNET	III	Event-free survivor
6	18	M	Ewing	II	Dead
7	15	M	Ewing	No surgery	Dead
8	34	M	Ewing/PNET	No surgery	Dead
9	38	M	Ewing	No surgery	Dead
10	17	M	Ewing/PNET	IV	Event-free survivor
11	31	M	Osteogenic	I	Event-free survivor
12	20	M	Osteogenic	III	Event-free survivor
13	27	F	Osteogenic	I	Event-free survivor
14	22	F	Osteogenic	II	Event-free survivor
15	14	M	Osteogenic	III	Event-free survivor
16	62	F	Osteogenic	No surgery	Dead
17	17	F	Osteogenic	II	Event-free survivor
18	15	F	Ewing	II	Event-free survivor
19	13	M	Osteogenic	IV	Event-free survivor
20	8	M	Osteogenic	IV	Event-free survivor

[a] Grade numbers, grading of chemotherapy response based on tumor necrosis (%). Grade I = <50%, II = 50–89%, III = 90–99%, IV = 100%.
[b] PNET, primitive neuroectodermal tumors.
[c] Dead, patient who showed no response or relapsed almost immediately after surgery and died.
[d] Event-free survivor, patient with no evidence of disease at time of latest follow-up.

Statistical Analysis. The statistical significance of each metabolite ratio as a prognostic marker was evaluated by predicting survival (EFSs *versus* those who died) using logistic regression and by predicting time-to-treatment-failure Cox proportional hazards regression. The NTP:P_i ratio was transformed by taking the square root to reduce the skewness of the statistical distribution, and an empirical cutoff of 0.65 was used to compare Kaplan-Meier disease-free survival curves for low *versus* high ratios.

RESULTS

Analysis of the ^{31}P NMR data suggested differences between pretreatment spectra in patients who had a complete clinical response and remained EFSs *versus* patients who did not respond, progressed locally or with distant metastases, and who all died shortly thereafter. Fig. 1 contains pretreatment spectroscopic data from a patient with ES. This patient has sustained an event-free survival for 44 months since neo-adjuvant chemotherapy followed by surgery. In this proton-decoupled spectrum, the phosphomonoesters PE and PC are resolved. The other peaks in the spectrum arise from P_i, phosphodiesters PDE [primarily glycerophosphocholine (GPC) and glycerophosphoethanolamine (GPE)] and high-energy metabolites NTPs and phosphocreatine (PCr). The PCr peak may have some contribution from muscle outside the voxel because of the point-spread function of the acquisition technique. The tumor shows highly elevated PE relative to PC. In contrast, Fig. 2 contains a pretreatment spectrum from a patient with ES who failed treatment and died later. This spectrum contains all of the peaks described above, but there is a lower level of high-energy phosphates and a higher level of P_i. The ratio of PE:PC is not as high as in the spectrum in Fig. 1*B*. In both of these patients, the tissue included in the voxel of interest was composed of both bone component and soft tissue component.

In Table 2, the average metabolite ratios and pH are shown for the patients who had complete clinical responses to the combination of

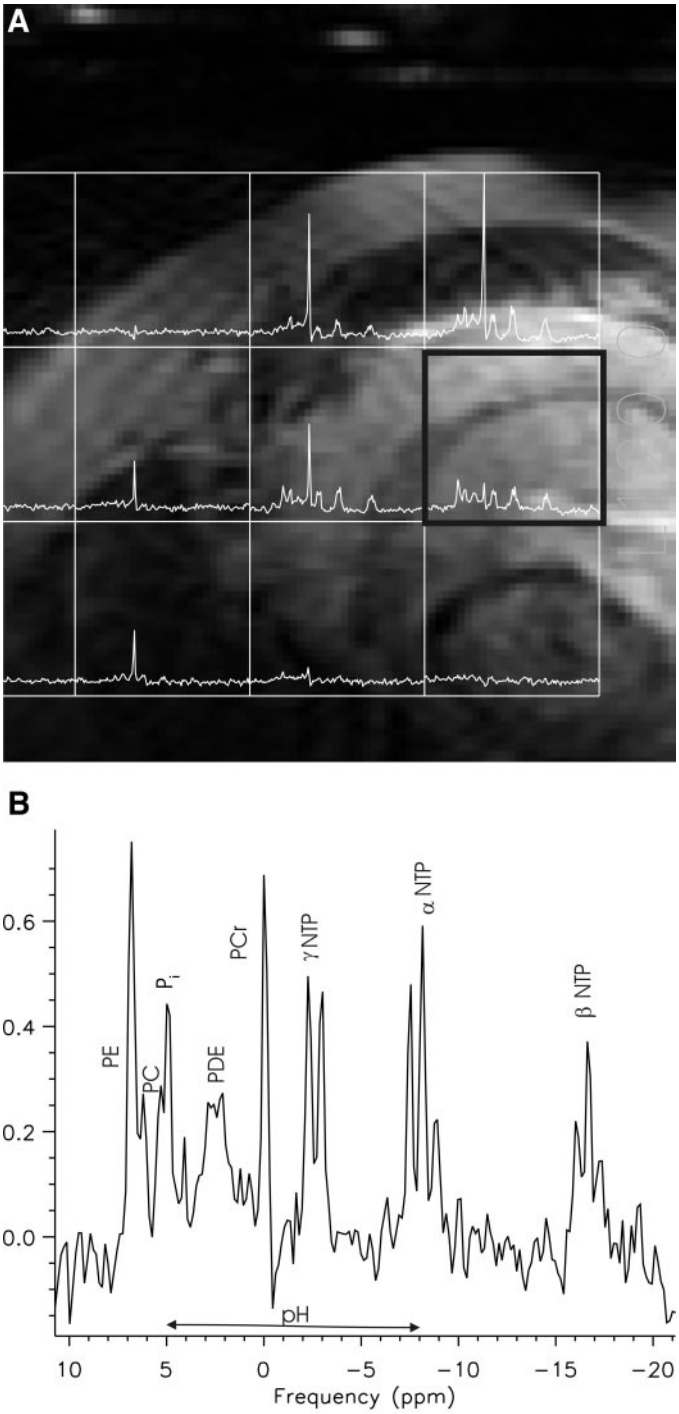

Fig. 1. Data from a patient with Ewing's sarcoma in the left thigh, who is an event-free survivor after 44 months after combined modality therapy. *A*, ^{31}P spectral grid superimposed on T_2-weighted fast spin-echo (FSE) axial image. *B*, pretreatment ^{31}P spectrum from tumor (*black box highlighted in A*). The peaks assigned in the spectrum are phosphoethanolamine (*PE*), phosphocholine (*PC*), inorganic phosphate (P_i), phosphodiesters (*PDEs*), phosphocreatine (*PCr*), and γ, α, β nucleotide triphosphate (*NTP*).

chemotherapy and surgery that were associated with durable event-free survival *versus* those who did not respond or responded briefly and died. PE and PC were resolved in 15 of 20 patients; the combined PME value is also reported. The only ratio that was a significant predictor of EFS was NTP:P_i ($P = 0.003$, by logistic regression on square root of the ratio). All of the patients who responded and were clinically free of disease 6 months after surgery remained in remission and are alive. Conversely, all of the patients who progressed or had brief responses died.

Fig. 3*A* shows the pretreatment NTP:P_i data in graphical form for the individual patients, demonstrating that there is some overlap between the two groups. In 1 of 7 patients in the group who died, the NTP:Pi ratio is higher than 0.65, and in 2 of 13 patients in the EFS group, the ratio is lower than 0.65, giving rise to an overlap in the data of Fig. 3*A*. The cutoff 0.65 has a sensitivity of 92% and specificity of 75% for predicting survival. Because there is some data on pH as a prognostic indicator in the literature, we show the pretreatment pH data for individual patients in Fig. 3*B*. In one patient, the pH could not be evaluated because the chemical shift of the α-NTP peak could not be determined because of poor signal:noise ratio.

Fig. 4 shows the Kaplan-Meier survival curve illustrating the relationship between pretreatment NTP:Pi and time to treatment failure. An empirical cutoff of 0.65 was used for grouping patients to display

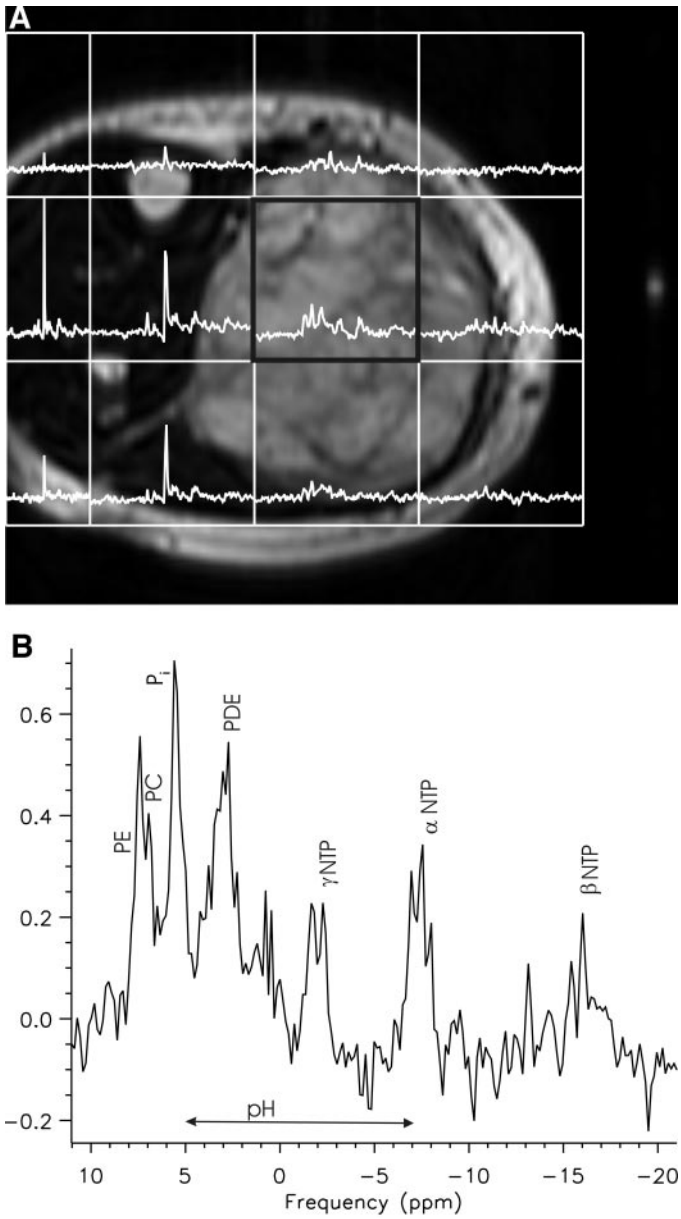

Fig. 2. Data from a patient with Ewing's sarcoma in the right calf, who failed combined modality therapy and died shortly thereafter. *A*, ^{31}P spectral grid superimposed on T_2-weighted fast spin-echo (FSE) axial image. *B*, pretreatment ^{31}P spectrum from tumor (*black box highlighted in A*). The peak assignments are the same as in Fig. 1*B*.

Table 2 *Pretreatment values (mean ± SEM) of nuclear magnetic resonance (NMR) parameters in patients who had event-free survival (EFS) versus those who died (D)*

	PE[a]:NTP	PE:PC	PME:NTP	PDE:NTP	PDE:PME	pH	NTP:P_i
EFS	1.09 ± 0.29	2.9 ± 1.02	1.51 ± 0.29	1.56 ± 0.28	1.34 ± 0.31	7.5 ± 0.06	1.12 ± 0.14
D	1.06 ± 0.25	2.25 ± 0.64	2.03 ± 0.36	2.68 ± 0.87	1.68 ± 0.53	7.33 ± 0.09	0.45 ± 0.09
P	0.91	0.60	0.29	0.26	0.59	0.15	0.003

[a] PE, phosphoethanolamine; NTP, nucleoside triphosphate; PC, phosphocholine; PME, phosphomonoester; PDE, phosphodiester; P_i, inorganic phosphate.

survival curves for lower and higher NTP:Pi ratios based on the data shown in Fig. 3*A*, *i.e.*, it appeared to provide the best separation. It is worth noting that if any other arbitrary value in the range 0.35–0.95 is used as a cutoff, a nominal *P* between 0.0001 and 0.011 is obtained, and the data are still significant. The survival analysis showed that NTP:Pi was a highly significant predictor ($P = 0.003$, based on the score test of the square root of the ratio as a continuous-valued covariate in Cox proportional hazards regression).

The individual normalized metabolite levels are not shown because there were no significant differences observed between the two groups. These data were more scattered and the SDs much larger than in the ratio data. This could be due to several factors. The various scaling factors necessary for individual metabolite quantitation may amplify interindividual differences in metabolites, increasing scatter and reducing significance. Also, although we attempted to limit the amount of necrotic-appearing tissue in the voxel, interpatient variations in the percentage of viable tissue could also affect individual metabolite quantitation, because little high-energy phosphate signal would be expected in necrotic tissue. Finally, the amount of bone tissue in the voxel could also change the metabolite levels. However, when the estimated percentage of soft tissue was compared with the individual metabolite levels, no correlation was observed.

In 12 of 20 patients, we were able to evaluate changes in NMR parameters that occurred between the pretreatment spectrum and a subsequent follow-up study done before the second cycle of treatment. The second exam was performed, on average, 15 ± 2 days after the start of treatment. The changes in the NMR parameters with treatment did not yield any information that predicted prognosis; however, the sample size was limited.

DISCUSSION

The data from the 20 patients in the current study indicate that a higher pretreatment ratio of high-energy phosphates to P_i (NTP:P_i) may be predictive of better outcome in bone sarcomas. This suggests that the energy status of these tumors influences patient prognosis. There is also previous data in the literature for soft tissue sarcomas supporting this hypothesis. A series of studies from the group at Duke University has investigated the relationship between tumor metabolism, hypoxia, and response to hyperthermia and radiation in soft tissue sarcomas (14–18). Pretherapy pH and water T_2 were shown to predict necrosis in human tumors (15, 18) with higher T_2 and/or higher pH correlating positively with percentage of necrosis at the time of surgical resection. When changes between pretreatment and follow-up studies were assessed, a decrease in NTP:PME correlated with >95% necrosis (15) and changes in NTP:P_i and PCr:P_i correlated negatively with percentage of necrosis at surgery (18). The present study differs from these prior investigations in several important respects. The data from the previous studies focused on soft tissue sarcomas, whereas the data presented here are based on patients with bone tumors (ES or OS). The prognosis for these tumors differs from those of soft tissue sarcomas; OSs typically are more responsive to

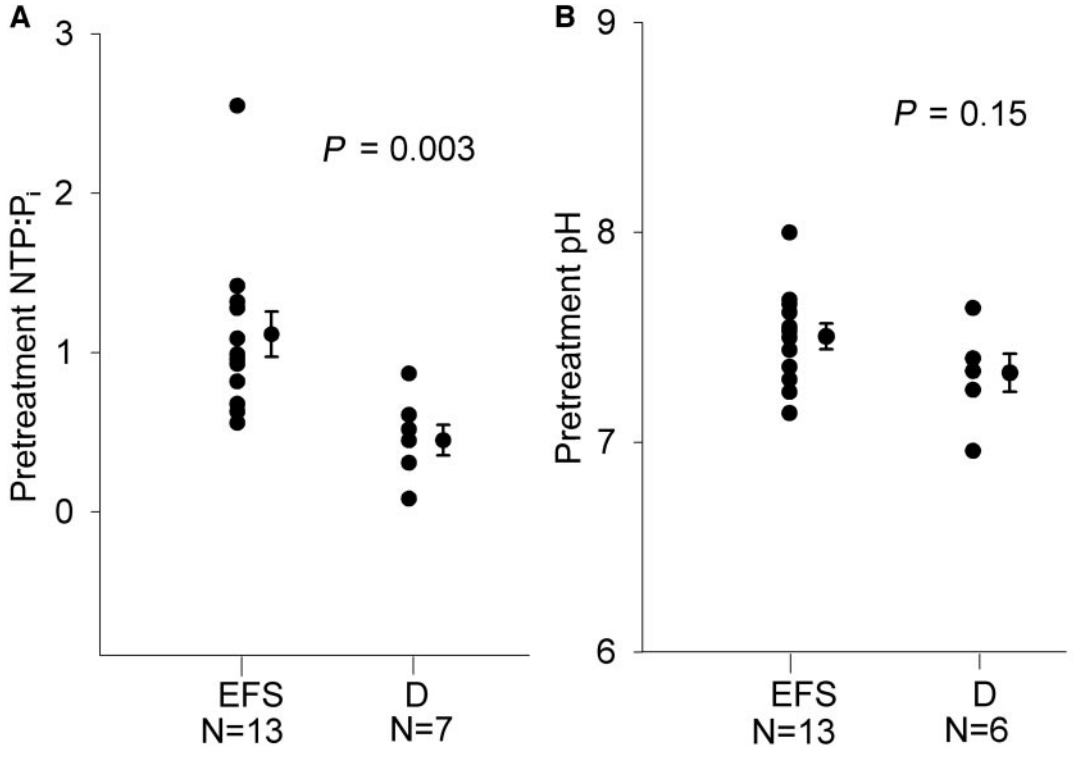

Fig. 3. *A*, Pretreatment nucleotide triphosphate:inorganic phosphate (*NTP:P_i*) ratios in bone sarcomas. The data are from 13 patients who had event-free survival (*EFS*) and 7 who died (*D*). *Circles with bars*, mean ± SEM. *B*, pretreatment pH values in bone sarcomas. The data are from 13 patients who had event-free survival and 6 who died. *Circles with bars*, mean ± SEM.

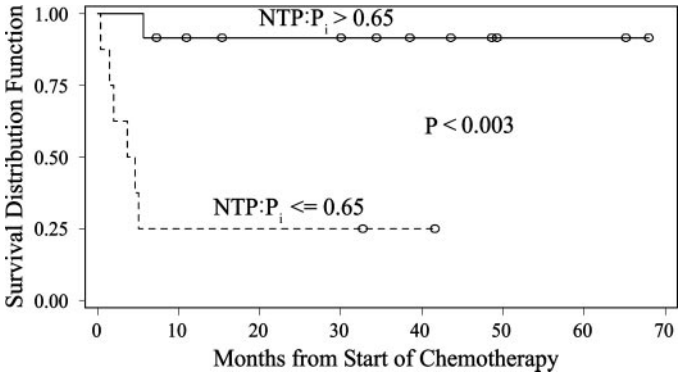

Fig. 4. Kaplan-Meier survival curve based on pretreatment nucleotide triphosphate: inorganic phosphate (*NTP:P$_i$*) *versus* time to treatment failure with the cutoff value of NTP:P$_i$ = 0.65. $P < 0.003$ is for square root of the ratio as a continuous-value covariate.

chemotherapy and have a better prognosis than soft tissue sarcomas. In addition, the patients in the prior studies received hyperthermia and radiation, whereas the patients studied here were treated with chemotherapy (in ES: cyclophosphamide, doxorubicin, vincristine, ifosfamide, etoposide; in OS: high dose methotrexate, cisplatin, doxorubicin, ifosfamide, etoposide). Despite these differences, it is noteworthy that in both studies, parameters related to energy metabolism were found to correlate with response, and patients whose tumors had higher energy levels before therapy had a better outcome. There is no literature available in preclinical models of bone tumors trying to predict response based on a single pretreatment spectrum. However, there are two preclinical studies (24, 25) wherein changes in PCr:P$_i$ predict a lack of tumor treatment response in human OS implanted into nude mice with a specificity of 70% and a sensitivity of 54%.

There has been much interest recently in tumor hypoxia as a prognostic indicator in human tumors. Oxygen-sensing microelectrodes have enabled investigators to directly measure oxygen levels in certain tumors accessible by the instrument. In soft tissue sarcomas, poorer oxygenation status has been correlated with the development of metastases and decreased disease-specific and overall survival (14, 26). Similarly, large numbers of studies have been performed in both cervical cancer (27–34) and head and neck cancers (35–42) showing poor outcome in patients with more hypoxic tumors. Brizel *et al.* (14) showed that PCr:P$_i$ as measured by ^{31}P NMR correlated with tumor hypoxia in soft tissue sarcomas. In addition, early animal studies on several tumor models indicated that pretreatment phosphorus-metabolite ratios (PCr:P$_i$, NTP:P$_i$) and pH are sensitive indices of tissue hypoxic fraction, well-perfused fraction, and tumor oxygenation status (43–50). Hence, ^{31}P NMR has the capability of providing a noninvasive measurement of energy status and also may be a surrogate of the related oxygenation status, making ^{31}P NMR a potential prognostic indicator.

The level of tumor lactate, which is generated by anaerobic glycolysis, has also been correlated with tumor oxygenation and, additionally, with patient outcome in cervical (51) and head and neck (11) cancers. Thus, another tumor-energy status marker has been linked with outcome. Interestingly, ATP, measured by bioluminescence, did not correlate with outcome in a study of advanced cervical cancer (50).

Energy status and hypoxia may influence patient outcome through several mechanisms. Radiotherapy is well known to be less effective in poorly oxygenated tumors and poor local tumor control leads to poor outcome (26, 52, 53). In addition, the hypoxic tumor microenvironment has been associated with the increased occurrence of genetic mutations. These mutations may result in the promotion of certain factors that make the tumor more likely to metastasize, and/or in the suppression of factors that prevent metastases (54). In addition, the stress induced by hypoxia has been reported to cause selection of cells that have a survival advantage under adverse conditions, and these cells may also have greater metastatic potential (55). With its capability of noninvasively assessing energy status and hypoxia, ^{31}P NMR spectroscopy has the potential to play a prognostic role in human cancer.

The disadvantages of ^{31}P MRSI include the requirement for specialized equipment, in addition to the need for "large voxels" because of the low sensitivity of the nucleus. In this study, the average voxel size was 27 $\pm$ 1.5 cm^3, which gave adequate signal:noise ratio in a 34-min scan for tumors that were 3–8 cm deep. Because of this large voxel size, it was usually feasible to obtain optimal data from only one voxel, centered within the coil sensitivity profile and achieving the highest signal:noise ratio possible at the tumor depth. Walenta *et al.* (51) have recently suggested that "macroscopic heterogeneities may not be as pronounced as heterogeneities in microscopic dimensions," which suggests that macroscopic biopsies (and possibly localized imaging data) may be more representative of the tumor. This has been seen in previous animal studies (46) using nonlocalized NMR measurements of tumor metabolism and bioluminescence techniques.

In the present study, we have used ^{1}H-decoupled ^{31}P MRSI to assess possible prognostic factors in bone sarcomas. In these tumors, the pretreatment NTP:P$_i$ ratio, an index of tumor bioenergetic status, exhibited different values in patients who subsequently responded well or poorly to combined treatment with chemotherapy and surgery. Because combined chemotherapy and surgery is the standard of care, we did not attempt to determine whether this methodology predicts response to either treatment alone. The patients that did not respond to combined therapy had a lower pretreatment NTP:P$_i$ ratio than the patients who did. Confirmation of these findings will require a prospective trial, but the preliminary results appear promising. The availability of a noninvasive pretreatment prognostic index would greatly facilitate the treatment planning of bone cancers.

REFERENCES

1. Link, M. P., Gebhardt, M., Pizzo, P. A., and Poplack, D. G. Osteosarcoma. *In:* Principles and Practice of Pediatric Oncology, Ed. 4. Philadelphia: Lippincott, Williams, & Wilkins, 2002.
2. Gurney, J. G, Swensen, A. R., Bulterys, M. Malignant bone tumors. *In:* L. A. G. Ries, M. A. Smith, J. G. Gurney, M. Linet, T. Tamra, J. L. Young, and G. R. Bunin (eds.), Cancer Incidence and Survival among Children and Adolescents: United States SEER Program 1975–1995, NIH Publ. No. 99-4649, pp. 99-110. Bethesda, MD: National Cancer Institute, SEER Program, 1999.
3. Dahlin, D. C., and Unni, K. K. Bone Tumors: General Aspects and Data on 8542 Cases, Ed. 4. Springfield, IL: Charles C. Thomas, 1986.
4. Provisor, A. J., Ettinger, L. J., Nachman, J. B., Krailo, M. D., Makley, J. T., Yunis, E. J., *et. al.* Treatment of non metastatic osteosarcoma of the extremity with preoperative and postoperative chemotherapy: a report from the Children's Cancer Group. J. Clin. Oncol., *15:* 76–84, 1997.
5. Rosen, G., Marcove, R. C., Huvos, A. G., Caparros, B I., Lane, J. M., and Nirenberg, A. Primary osteogenic sarcoma: eight-year experience with adjuvant chemotherapy. J. Cancer Res. Clin. Oncol., *106* (Suppl.)*:* 55–67, 1983.
6. Wunder, J. S., Paulian, G., Huvos, A. G., Heller, G., Meyers, P. A., and Healey, J. H. The histological response to chemotherapy as a predictor of the oncological outcome of operative treatment of Ewing sarcoma. J. Bone Joint Surg. Am., *80:* 1020–1033, 1998.
7. Bielack, S. S., Kempf-Bielack, B., Delling, G., Exner, G. U., Flege, S., Helmke, K., Kotz, R., Salzer-Kuntschik, M., Werner, M., Winkelmann, W., Zoubek, A., Jurgens, H., and Winkler, K. Prognostic factors in high-grade osteosarcoma of the extremities or trunk: an analysis of 1,702 patients treated on neoadjuvant cooperative osteosarcoma study group protocols. J. Clin. Oncol., *20:* 776–790, 2002.
8. de Alava, E., Antonescu, C. R., Panizo, A., Leung, D., Meyers, P. A., Huvos, A. G., Pardo-Mindan, F. J., Healey, J. H., and Ladanyi, M. Prognostic impact of P53 status in Ewing sarcoma. Cancer (Phila.), *89:* 783–792, 2000.
9. Adam, M. F., Gabalski, E. C., Bloch, D. A., Oehlert, J. W., Brown, J. M., Elsaid, A. A., Pinto, H. A., and Terris, D. J. Tissue oxygen distribution in head and neck cancer patients. Head Neck, *21:* 146–153, 1999.
10. Star-Lack, J. M., Adalsteinsson, E., Adam, M. F., Terris, D. J., Pinto, H. A., Brown, J. M., and Spielman, D. M. *In vivo* ^{1}H MR spectroscopy of human head and neck lymph node metastasis and comparison with oxygen tension measurements. Am. J. Neuroradiol., *21:* 183–193, 2000.
11. Brizel, D. M., Schroeder, T., Scher, R. L., Walenta, S., Clough, R. W., Dewhirst, M. W., and Mueller-Klieser, W. Elevated tumor lactate concentrations predict for an increased risk of metastases in head-and-neck cancer. Int. J. Radiat. Oncol. Biol. Phys., *51:* 349–353, 2001.

12. Griffiths, J. R., Tate, A. R., Howe, F. A., and Stubbs, M. Magnetic resonance spectroscopy of cancer-practicalities of multi-centre trials and early results in non-Hodgkin's lymphoma. Eur. J. Cancer, *38:* 2085–2093, 2002.
13. Shukla-Dave, A., Poptani, H., Loevner, L. A., Mancuso, A., Serrai, H., Rosenthal, D. I., Kilger, A. M., Nelson, D. S., Zakian, K. L., Arias-Mendoza, F., Rijpkema, M., Koutcher, J. A., Brown, T. R., Heerschap, A., and Glickson, J. D. Prediction of treatment response of head and neck cancers with P-31 MR spectroscopy from pretreatment relative phosphomonoester levels. Acad. Radiol., *9:* 688–694, 2002.
14. Brizel, D. M., Scully, S. P., Harrelson, J. M., Layfield, L. J., Dodge, R. K., Charles, H. C., Samulski, T. V., Prosnitz, L. R., and Dewhirst, M. W. Radiation therapy and hyperthermia improve the oxygenation of human soft tissue sarcomas. Cancer Res., *56:* 5347–5350, 1996.
15. Sostman, H. D., Prescott, D. M., Dewhirst, M. W., Dodge, R. K., Thrall, D. E., Page, R. L., Tucker, J. A., Harrelson, J. M., Reece, G., Leopold, K. A., *et al.* MR imaging and spectroscopy for prognostic evaluation in soft-tissue sarcomas. Radiology, *190:* 269–275, 1994.
16. Prescott, D. M., Charles, H. C., Sostman, H. D., Dodge, R. K., Thrall, D. E., Page, R. L., Tucker, J. A., Harrelson, J. M., Leopold, K. A., Oleson, J. R., *et al.* Therapy monitoring in human and canine soft tissue sarcomas using magnetic resonance imaging and spectroscopy. Int. J. Radiat. Oncol. Biol. Phys., *28:* 415–423, 1994.
17. Sostman, H. D., Charles, H. C., Rockwell, S., Leopold, K., Beam, C., Madwed, D., Dewhirst, M., Cofer, G., Moore, D., Burn, R., *et al.* Soft-tissue sarcomas: detection of metabolic heterogeneity with P-31 MR spectroscopy. Radiology, *176:* 837–843, 1990.
18. Dewhirst, M. W., Sostman, H. D., Leopold, K. A., Charles, H. C., Moore, D., Burn, R. A., Tucker, J. A., Harrelson, J. M., and Oleson, J. R. Soft-tissue sarcomas: MR imaging and MR spectroscopy for prognosis and therapy monitoring. Work in progress. Radiology, *174:* 847–853, 1990.
19. Brown, T. R., Kincaid, B. M., and Ugurbil, K. NMR chemical shift imaging in three dimensions. Proc. Natl. Acad. Sci. USA, *79:* 3523–3526, 1982.
20. Vanhamme, L., van den Boogaart, A., and Van Huffel, S. Improved method for accurate and efficient quantification of MRS data with use of prior knowledge. J. Magn. Reson., *129:* 35–43, 1997.
21. Naressi, A., Couturier, C., Castang, I., de Beer, R., and Graveron-Demilly, D. Java-based graphical user interface for MRUI, a software package for quantitation of *in vivo*/medical magnetic resonance spectroscopy signals. Comput. Biol. Med., *31:* 269–286, 2001.
22. Murphy-Boesch, J., Jiang, H., Stoyanova, R., and Brown, T. R. Quantification of phosphorus metabolites from chemical shift imaging spectra with corrections for point spread effects and B1 inhomogeneity. Magn. Reson. Med., *39:* 429–438, 1998.
23. Kooby, D. A., Zakian, K. L., Challa, S. N., Matei, C., Petrowsky, H., Yoo, H. H., Koutcher, J. A., and Fong, Y. Use of phosphorous-31 nuclear magnetic resonance spectroscopy to determine safe timing of chemotherapy after hepatic resection. Cancer Res., *60:* 3800–3806, 2000.
24. Kang, H., Ballinger, J. R., Sweeney, C., Croker, B. P., and Scott, K. N. ^{31}P changes as a measure of therapy response in human osteosarcomas implanted into nude mice. Magn. Reson. Imaging, *12:* 935–943, 1994.
25. Ballinger, J. R., Kang, H., Sweeney, C. A., Scott, J. D., Croker, B. P., and Scott, K. N. P-31 changes as a measure of therapy response in resistant and sensitive osteosarcomas implanted into nude mice. Magn. Reson. Imaging, *13:* 877–883, 1995.
26. Nordsmark, M., Alsner, J., Keller, J., Nielsen, O. S., Jensen, O. M., Horsman, M. R., and Overgaard, J. Hypoxia in human soft tissue sarcomas: adverse impact on survival and no association with p53 mutations. Br. J. Cancer, *84:* 1070–1075, 2001.
27. Hockel, M., Knoop, C., Schlenger, K., Vorndran, B., Baussmann, E., Mitze, M., Knapstein, P. G., and Vaupel, P. Intratumoral pO2 predicts survival in advanced cancer of the uterine cervix. Radiother. Oncol., *26:* 45–50, 1993.
28. Hockel, M., Vorndran, B., Schlenger, K., Baussmann, E., and Knapstein, P. G. Tumor oxygenation: a new predictive parameter in locally advanced cancer of the uterine cervix. Gynecol. Oncol., *51:* 141–149, 1993.
29. Hockel, M., Schlenger, K., Aral, B., Mitze, M., Schaffer, U., and Vaupel, P. Association between tumor hypoxia and malignant progression in advanced cancer of the uterine cervix. Cancer Res., *56:* 4509–4515, 1996.
30. Sundfor, K., Lyng, H., and Rofstad, E. K. Tumour hypoxia and vascular density as predictors of metastasis in squamous cell carcinoma of the uterine cervix. Br. J. Cancer, *78:* 822–827, 1998.
31. Fyles, A. W., Milosevic, M., Wong, R., Kavanagh, M. C., Pintilie, M., Sun, A., Chapman, W., Levin, W., Manchul, L., Keane, T. J., and Hill, R. P. Oxygenation predicts radiation response and survival in patients with cervix cancer. Radiother. Oncol., *48:* 149–156, 1998.
32. Knocke, T. H., Weitmann, H. D., Feldmann, H. J., Selzer, E., and Potter, R. Intratumoral pO2-measurements as predictive assay in the treatment of carcinoma of the uterine cervix. Radiother. Oncol., *53:* 99–104, 1999.
33. Haensgen, G., Krause, U., Becker, A., Stadler, P., Lautenschlaeger, C., Wohlrab, W., Rath, F. W., Molls, M., and Dunst, J. Tumor hypoxia, p53, and prognosis in cervical cancers. Int. J. Radiat. Oncol. Biol. Phys., *50:* 865–872, 2001.
34. Pitson, G., Fyles, A., Milosevic, M., Wylie, J., Pintilie, M., and Hill, R. Tumor size and oxygenation are independent predictors of nodal diseases in patients with cervix cancer. Int. J. Radiat. Oncol. Biol. Phys., *51:* 699–703, 2001.
35. Nordsmark, M., Overgaard, M., and Overgaard, J. Pretreatment oxygenation predicts radiation response in advanced squamous cell carcinoma of the head and neck. Radiother. Oncol., *41:* 31–39, 1996.
36. Brizel, D. M., Sibley, G. S., Prosnitz, L. R., Scher, R. L., and Dewhirst, M. W. Tumor hypoxia adversely affects the prognosis of carcinoma of the head and neck. Int. J. Radiat. Oncol. Biol. Phys., *38:* 285–289, 1997.
37. Stadler, P., Becker, A., Feldmann, H. J., Hansgen, G., Dunst, J., Wurschmidt, F., and Molls, M. Influence of the hypoxic subvolume on the survival of patients with head and neck cancer. Int. J. Radiat. Oncol. Biol. Phys., *44:* 749–754, 1999.
38. Brizel, D. M., Dodge, R. K., Clough, R. W., and Dewhirst, M. W. Oxygenation of head and neck cancer: changes during radiotherapy and impact on treatment outcome. Radiother. Oncol., *53:* 113–117, 1999.
39. Vanselow, B., Eble, M. J., Rudat, V., Wollensack, P., Conradt, C., and Dietz, A. Oxygenation of advanced head and neck cancer: prognostic marker for the response to primary radiochemotherapy. Otolaryngol. Head Neck Surg., *122:* 856–862, 2000.
40. Rudat, V., Vanselow, B., Wollensack, P., Bettscheider, C., Osman-Ahmet, S., Eble, M. J., and Dietz, A. Repeatability and prognostic impact of the pretreatment pO(2) histography in patients with advanced head and neck cancer. Radiother. Oncol., *57:* 31–37, 2000.
41. Nordsmark, M., and Overgaard, J. A confirmatory prognostic study on oxygenation status and loco-regional control in advanced head and neck squamous cell carcinoma treated by radiation therapy. Radiother. Oncol., *57:* 39–43, 2000.
42. Rudat, V., Stadler, P., Becker, A., Vanselow, B., Dietz, A., Wannenmacher, M., Molls, M., Dunst, J., and Feldmann, H. J. Predictive value of the tumor oxygenation by means of pO2 histography in patients with advanced head and neck cancer. Strahlenther. Onkol., *177:* 462–468, 2001.
43. Evelhoch, J. L., Sapareto, S. A., Nussbaum, G. H., and Ackerman, J. J. Correlations between ^{31}P NMR spectroscopy and ^{15}O perfusion measurements in the RIF-1 murine tumor *in vivo*. Radiat. Res., *106:* 122–131, 1986.
44. Okunieff, P., Ramsay, J., Tokuhiro, T., Hitzig, B. M., Rummeny, E., McFarland, E., Neuringer, L. J., and Suit, H. Estimation of tumor oxygenation and metabolic rate using ^{31}P MRS: correlation of longitudinal relaxation with tumor growth rate and DNA synthesis. Int. J. Radiat. Oncol. Biol. Phys., *14:* 1185–1195, 1988.
45. Vaupel, P., Okunieff, P., Kallinowski, F., and Neuringer, L. J. Correlations between ^{31}P-NMR spectroscopy and tissue O_2 tension measurements in a murine fibrosarcoma. Radiat. Res., *120:* 477–493, 1989.
46. Mueller-Klieser, W., Schaefer, C., Walenta, S., Rofstad, E. K., Fenton, B. M., and Sutherland, R. M. Assessment of tumor energy and oxygenation status by bioluminescence, nuclear magnetic resonance spectroscopy, and cryospectrophotometry. Cancer Res., *50:* 1681–1685, 1990.
47. Sostman, H. D., Rockwell, S., Sylvia, A. L., Madwed, D., Cofer, G., Charles, H. C., Negro-Vilar, R., and Moore, D. Evaluation of BA1112 rhabdomyosarcoma oxygenation with microelectrodes, optical spectrophotometry, radiosensitivity, and magnetic resonance spectroscopy. Magn. Reson. Med., *20:* 253–267, 1991.
48. Wendland, M. F., Iyer, S. B., Fu, K. K., Lam, K. N., and James, T. L. Correlations between *in vivo* ^{31}P MRS measurements, tumor size, cell survival, and hypoxic fraction in the murine EMT6 tumor. Magn. Reson. Med., *25:* 217–232, 1992.
49. Okunieff, P. G., Koutcher, J. A., Gerweck, L., McFarland, E., Hitzig, B., Urano, M., Brady, T., Neuringer, L., and Suit, H. D. Tumor size dependent changes in a murine fibrosarcoma: use of *in vivo* ^{31}P NMR for non-invasive evaluation of tumor metabolic status. Int. J. Radiat. Oncol. Biol. Phys., *12:* 793–799, 1986.
50. Gerweck, L. E., Urano, M., Koutcher, J., Fellenz, M. P., and Kahn, J. Relationship between energy status, hypoxic cell fraction, and hyperthermic sensitivity in a murine fibrosarcoma. Radiat. Res., *117:* 448–458, 1989.
51. Walenta, S., Wetterling, M., Lehrke, M., Schwickert, G., Sundfor, K., Rofstad, E. K., and Mueller-Klieser, W. High lactate levels predict likelihood of metastases, tumor recurrence, and restricted patient survival in human cervical cancers. Cancer Res., *60:* 916–921, 2000.
52. Koutcher, J. A., Alfieri, A. A., Devitt, M. L., Rhee, J. G., Kornblith, A. B., Mahmood, U., Merchant, T. E., and Cowburn, D. Quantitative changes in tumor metabolism, partial pressure of oxygen, and radiobiological oxygenation status postradiation. Cancer Res., *52:* 4620–4627, 1992.
53. Schlenger, K., Hockel, M., Mitze, M., Schaffer, U., Weikel, W., Knapstein, P. G., and Lambert, A. Tumor vascularity—a novel prognostic factor in advanced cervical carcinoma. Gynecol. Oncol., *59:* 57–66, 1995.
54. Rofstad, E. K. Microenvironment-induced cancer metastasis. Int. J. Radiat. Biol., *76:* 589–605, 2000.
55. Graeber, T. G., Osmanian, C., Jacks, T., Housman, D. E., Koch, C. J., Lowe, S. W., and Giaccia, A. J. Hypoxia-mediated selection of cells with diminished apoptotic potential in solid tumours. Nature (Lond.), *379:* 88–91, 1996.

53. Schlenger, K., Hockel, M., Mitze, M., Schaffer, U., Weikel, W., Knapstein, P. G., and Lambert, A. Tumor vascularity—a novel prognostic factor in advanced cervical carcinoma. Gynecol. Oncol., *59:* 57–66, 1995.
54. Rofstad, E. K. Microenvironment-induced cancer metastasis. Int. J. Radiat. Biol., *76:* 589–605, 2000.
55. Graeber, T. G., Osmanian, C., Jacks, T., Housman, D. E., Koch, C. J., Lowe, S. W., and Giaccia, A. J. Hypoxia-mediated selection of cells with diminished apoptotic potential in solid tumours. Nature (Lond.), *379:* 88–91, 1996.